

Role of Multi-Detector Computed Tomography in Evaluation of Ankle Trauma

Medhat M. Refaat, Ahmed S. Ali, Amr M. Riyadh

Department of Radio-Diagnosis and Medical Imaging, Faculty of Medicine, Benha University, Egypt.

Corresponding to: Dr. Amr M. Riyadh, Department of Radio-Diagnosis and Medical Imaging, Benha Faculty of Medicine, Benha University, Egypt.

Email:
amrriyadh2021@gmail.com

Received: 20 August 2021

Accepted: 2 August 2022

Abstract:

Background: Injuries to the foot and ankle are often missed or underestimated during the initial care for poly-traumatized patients. **Aim:** to evaluate the role of MDCT in evaluation of osseous injuries of the ankle. **Methods:** The present work included sixty patients. All patients were recommended for CT evaluation after being examined by a plain X-ray to further evaluate already diagnosed or exclude ankle and hind foot osseous injuries. All patients were examined using 6 and 16 multi-detector CT scanners. **Results:** The present study included 20 malleolar, 18 Pilon fractures, 15 talar fractures, and 23 calcaneal fractures. Six patients (9%) had multiple fractures of the ankle region. Five patients (7.5%) of which had Pilon and talar fractures, and one (1.5%) had calcaneal and malleolar fractures. MDCT allows for scanning through full plaster casts or back-slabs. Eighteen patients constituting 23.7% presented with distal tibial fracture (Pilon fracture). **Conclusion:** Computed tomography is valuable in the diagnosis of cases of occult syndesmotic injury, especially when the patient cannot tolerate stress radiographs. MDCT is recommended if an intra-articular fracture or major displacement is suspected. This allows for a three-dimensional analysis of fracture morphology and determination of joint involvement and is extremely helpful in planning the surgical approach.

Keywords: Multi-Detector CT; Ankle; Trauma

Introduction

The ankle is one of the most injured joints in the human body. Although many of these injuries are purely ligamentous, fractures are not infrequent (1).

The rate of ankle fractures has increased significantly in many industrialized countries, most likely due to growth in the number of people involved in athletics and in the size of the elderly population (2).

Axial CT images alone can be difficult to interpret the complex anatomy of the ankle and foot (3).

The development of multi-detector CT (MDCT) has transformed CT from a simple, cross-sectional imaging technique to an advanced, three-dimensional (3-D) imaging modality, enabling excellent 3-D displays. Its advantages over its

predecessor, single-slice helical CT, are increased speed and coverage, isotropic imaging capability, reduced metallic artifacts, and ease of interpretation (4).

Radiography often underestimates the extent of injury and degree of displacement of fracture fragments in the extremities. MDCT in the extremities is helpful in fracture detection, evaluation, characterization, and treatment planning. Complex intra-articular fractures of the extremities can also be evaluated thoroughly (4). Multi-detector CT scanning is associated with a substantial gain in performance and decreased scan times. Reduced scan times and motion artifacts are valuable in the evaluation of musculo-skeletal trauma, especially in pediatric patients (4).

The aim of the work was to study the value of MDCT in evaluation of osseous injuries of the ankle region.

Patients and methods

This cross-sectional study, included sixty seven patients suffering from known or suspected ankle osseous injuries, referred to radiological department at Benha university hospital, during the period from March 2020 to March 2021.

This study was approved by the Ethical Committee of Benha Faculty of Medicine, and a written consent was taken from all subjects before enrolment of the study.

Inclusion criteria:

Known or suspected ankle osseous injuries.

Exclusion criteria:

- Pregnancy.
- Post-operative cases with metallic implants.

All the studied patients were subjected to the following:

1. Full history taking.
2. Thorough clinical examination.
3. Plain X-ray of the ankle and foot.
4. The medical ethics were considered: the patient was aware of the examination; patient agreement was obtained, and the patient had to get benefit from the examination.
5. Non enhanced MDCT of the ankle and foot with:
 - Multi-planar volume reformation (MPR).
 - Three-dimensional VR.

Patient positioning:

- The patient lies supine with the unaffected limb bent at the knee to exclude it from the scan plane.
- The affected limb should be positioned at the center of the gantry with the leg extended and the ankle placed in the neutral position.
- Plaster cast was not needed to be removed before the examination.

Scan parameters:

The examinations were done on Siemens 6 scanner and 16 Philips MDCT. Scanning parameters were: 250 mAs, 120 KVP, tube rotation time of 0.6 s/rot., 2 mm slice thickness and 1 mm reconstruction increment for Philips MDCT, while for Siemens these were: 150 mAs, 120 KVP, 0.8 s/rot., 1 mm slice thickness and 0.5 mm reconstruction increment.

Reconstruction methods:

The MDCT images were reconstructed using filtered reconstruction algorithms. The thin slices were sent to the workstation, after reconstruction of the raw data using sharp bony (B70) and smooth soft tissue reconstruction algorithms (B30), where they were

available to view in axial, sagittal and coronal planes. Volume rendering techniques were displayed in all patients for further clarification and for planning for surgical interference.

Statistical analysis:

The collected data analyzed using SPSS software qualitative data expressed as number and percentage while quantitative data expressed as mean \pm SD. Suitable statistical tests of significance calculated. *P* value less than 0.05 significant.

Results

This study included 67 patient (70 feet and 76 fracture type) suffering from unilateral or bilateral ankle region fractures as sequel of trauma (the two main injury mechanisms were falling from a height and a traffic accident). All patients were recommended for CT evaluation after being examined by a plain X-ray to further evaluate already diagnosed or exclude

ankle and hind foot osseous injuries. From the 67 patients, 64 had unilateral fracture, 3 had bilateral injuries and 6 had combined (more than one fractures region) bringing our total number of cases to 76. Of the 67 patients, 79% were men ($n= 46$). The mean age of the study group was 35 years (range of age 13 – 74 years). Of the 67 patients, there were 6 patients (9%) with multiple fractures in more than one region. Of which five patients (7.5%) had distal tibial and talar fractures, and one (1.5%) had calcaneal and malleolar fractures (Table 1).

From the total of 76 fracture, 23 presents with calcaneal fracture, 20 with ankle fracture ,18 with Pilon fracture and 15 patients with talus fracture. The number of the patients and number of fractures according to anatomic location are shown in table 2.

Table 1: Distribution of patients according to age.

Age in years	Number of patients	Percentage
10-19	9	13.4 %
20-29	11	16.4 %
30-39	26	38.8 %
40-49	10	14.9 %
50-59	8	11.9 %
60-	3	0.4 %
Total	67	100 %

Table 2: Number of patients and number of fractures related to anatomic location.

Location	Fracture	
	Number	%
Malleolar	20	26.3
Pilon	18	23.7
Talus	15	19.7
Calcaneus	23	30.3

In the present study, malleolar fractures were present in 20 feet. Of which, 13 patients presented with Weber B, Lauge Hansen SE type of injury and 6 presented with Weber C, Lauge Hansen PE type of injury and 1 presented with Weber C, Lauge Hansen PA type of injury. From the 13 patients with Weber B, Lauge Hansen SE type of injury, six patients were diagnosed as stage 3, six as stage 4 and one patient as stage 2. All the 6 patients with Weber C, Lauge Hansen PE type of injury were diagnosed as stage 4 (Table 3). Of the 20 malleolar fractures, 19 fractures were unstable and 1 was stable. Instability was attributed in patients due to fractures involving both sides of the ankle mortise causing the ring to be broken in two places either by fracture or ligamentous injury, two patients who were diagnosed as Weber C fractures, the fibular fracture was highly positioned which was seen only in the scout film. Two patients that were diagnosed as Lauge Hansen PE type of injury stage 4, although no medial malleolar fracture could be detected, yet edema and high signal fluid intensities were detected at the site of the deltoid ligament denoting its injury (Table 4).

In our study, eighteen patients constituting 23.7% presented with distal tibial fracture (Pilon fracture). The new classification proposed by Leonetti divided the pilon fracture in 4 groups according to the number of the fragments at the joint level. Therefore, non-displaced fractures or extra-articular fractures (1 articular fragment) were included in group I. Two parts fractures were included in group II, 3 parts fractures in group III and 4 parts and comminuted fractures were included in group IV. Accordingly, in our study using this new classification, two patients were diagnosed as type I, one patient as type II, three patients as type III and six patients as type IV (Table 5).

Table 3: weber classification of the 20 malleolar fractures.

CT findings	Number of patients	Percentage
Weber B	13	65%
Weber C	7	35%
Total	20	100%

Table 4: Lauge Hansen **classification** of the 20 malleolar fractures.

CT findings	Number of patients	Percentage
Lauge Hansen SE type stage 3	13	65%
Lauge Hansen PE type stage 4	6	30%
Lauge Hansen PA	1	5%
Total	20	100%

Associated fibular fracture was a common finding in association with Pilon fractures which was seen in nine patients (50 %) in our study, six of which were in association with type IV, two patients with type I and one patient with type III. Three patients of the eighteen patients were associated with talar body fracture, one as crushed body fracture, another as lateral process and the other as posterior process fracture. Two patients had articular incongruity and tibio-talar dislocation. The CT demonstrated well the degree of articular comminution and incongruity (Table 5).

In our study, fifteen patients constituting 19.7% presented with talar fractures, of which six fractures involved the posterior process, five fractures involved the body, three fractures involved the talar neck and only one fracture involved the lateral process (Table 6).

Of the six patients presented with posterior process fracture, three of them presented by lateral tubercle fracture (Shepherd fracture) and two presented by medial tubercle fracture (Cedell fracture) while one patient presented by fracture of both tubercles. Of the five patients with body fractures, two of them presented by central body simple shear fracture, one with central body comminuted fracture with

few fragments, one with central body crushed comminuted fracture with multiple fragments and one by osteochondral dome fracture. Of the three talar neck fractures, two patients classified as Hawkin's type I while the third patient classified as Hawkins's type III. Only one patient presented with lateral process fracture, showing intra-articular extension. Articular involvement of the fractures was identified in 10 out of 15 patients, ankle (tibiotalar) joint involvement was present in five patients and subtalar joint involvement was present in ten patients as there were five patients showing extension to both joints, yet none showed talonavicular joint involvement. Two patients presented dislocation of both subtalar and ankle joints, one of them presented by crushed comminuted fracture of the body while the other presented with Hawkin's type III talar neck fracture. The coronal MPR image was used to assess involvement of the ankle joint and congruity of the talo-tibial articular surface. It was also helpful to identify extension of fractures to the subtalar articulation and incongruity of the posterior subtalar facet.

The axial image was the key to evaluate the talo-navicular articulation and to identify any osteo-chondral involvement

of this region. The sagittal image was the best to evaluate alignment of the posterior subtalar joint and depicted the dislocated joint in one patient. Twenty patients had calcaneal fractures, three patients (15%) of them presented with bilateral calcaneal fractures. Of these 20 patients, falling from height was the mechanism of injury in 15 patients (75%), while traffic accidents

were the mechanism of injury in 5 patients (25%). There were twenty-three calcaneal fractures, classified as Sanders type I in 1 patient (4.3 %), Sanders type II in 10 patients (43.5%), sanders type III in 10 patients (43.5%) and Sanders type IV in 2 patients (8.7%) (Table 7).

Table 5: Distribution of Pilon fractures according to the new classification.

Classification		Number of fractures	Percentage
Type I	I b	2	11.1%
type II	II f	1	5.5 %
	III f	1	5.5 %
type III	III s	2	11.1 %
	Four parts fracture	4	22.2 %
type IV	Anterior commination	2	11.1 %
	Medial commination	6	33.3 %
	Total	18	100%

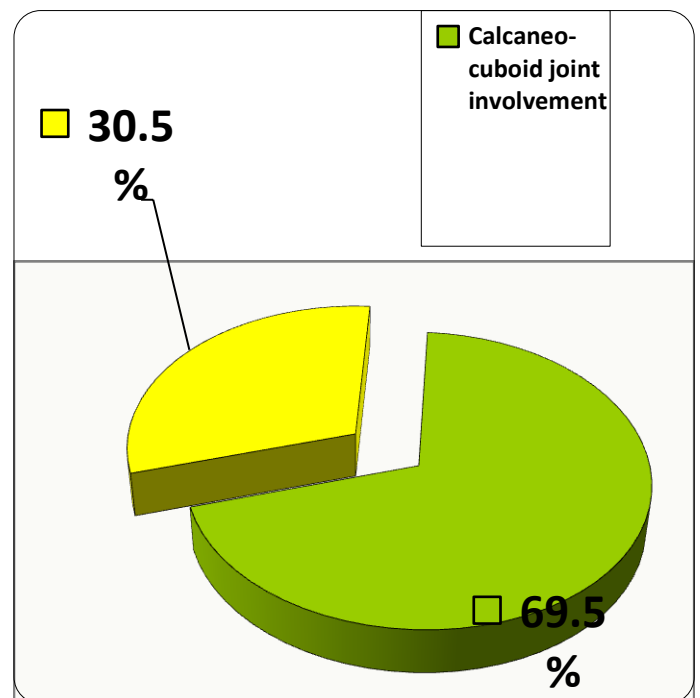
Table 6: Distribution of talus fractures.

CT findings	Number of patients	Percentage
Head	0	0%
Neck	3	20%
Body	5	33%
Posterior process	6	40%
Lateral process	1	7%
Total	15	100%

Table 7: Distribution of calcaneal fractures according to Sanders classification.

Type of calcaneal fracture	Classification	Number of fractures	Percentage
	Sanders type I	1	4.3%
	IIA	7	30.4%
	Sanders type II		
	IIB	2	8.7%
	IIC	1	4.3 %
<i>Intra-articular fracture</i>	IIIAB	8	34.8%
	Sanders type III		
	IIIAC	2	8.7
	IIIBC	0	0%
	Sanders type IV	2	8.7%
Total		23	100%

Classification was done on basis of axial and coronal images oriented parallel to the posterior facet of the sub-talar joint as shown on the sagittal MPR image. The coronal MPR image was the key to depict the number and location of intra-articular fracture lines as well as the degree of displacement of articular fragments, and to finally classify calcaneal fractures. Of the 23 feet showing calcaneal fractures, calcaneo-cuboid joint involvement was present in 16 feet accounting for 69.5 %. Calcaneo-cuboid joint involvement was best identified in the axial image with adequate depiction of the degree of articular incongruity if any, which has a significant influence on the long-term outcome of fracture healing (fig.1).

**Figure 1:** Distribution of calcaneal fractures according to calcaneo-cuboid joint involvement.

Case 1: fig. 2, clinical presentation: A 28-year-old female patient presented by left ankle pain and swelling due to motor vehicle accident. **Diagnosis:** Tri-malleolar fracture of the left ankle involving the tibio-fibular syndesmosis with ankle instability (Weber B, Lauge Hansen SER type of injury-stage IV).

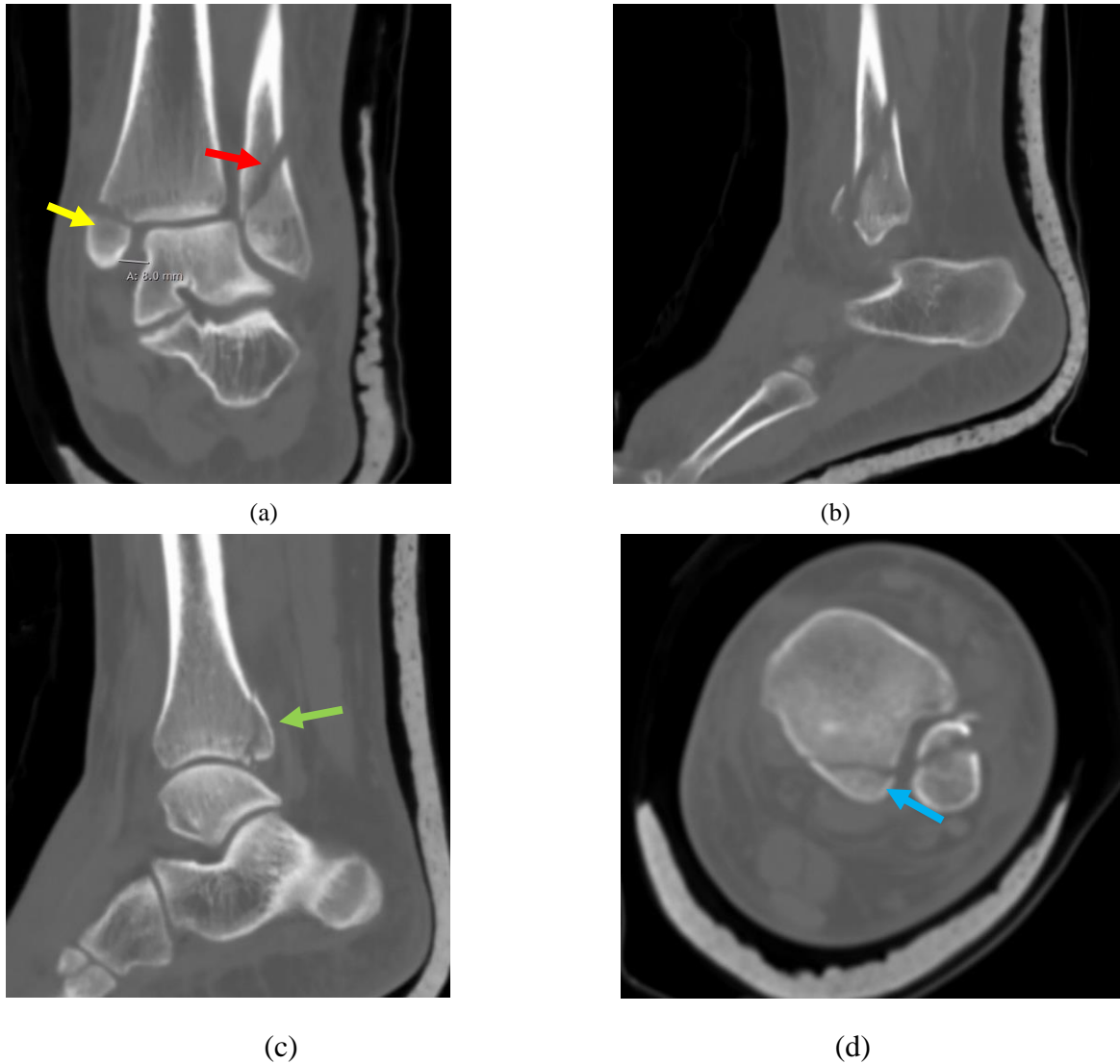


Figure: case 1

- Coronal reformatted CT image (a) demonstrates oblique fracture of the distal fibula at the level of the ankle syndesmosis (red arrows) as well as the avulsion fracture of the medial malleolus (yellow arrow) with evident widened medial clear space
- Sagittal reformatted CT image (b) demonstrate a spiral distal fibular fracture
- Sagittal reformatted CT image (c) demonstrates the posterior malleolus fracture
- Axial multi-detector image (d) demonstrates avulsion of the posterior attachment of the inferior tibio-fibular syndesmosis (posterior malleolus) (blue arrow).

Case 2: fig. 3, clinical presentation: A 55-year-old male presented by left ankle pain and swelling due to motor vehicle accident. **Diagnosis:** Posterior malleolus avulsion fracture and proximal fibular fracture with widened ankle syndesmosis (Weber C, Lauge Hansen PER type of injury-stage IV)



Figure: case 2

- Sagittal reformatted CT image (a) demonstrates posterior malleolus fracture
- Axial CT image (b) of the distal tibia demonstrates well the avulsion fracture of the posterior malleolus with widened lateral clear space (measuring 6 mm)
- 3D volume rendering image(c) demonstrates well the posterior malleolus fracture
- Coronal reformatted CT image (d) demonstrates no evidence of any fracture of the distal fibula and intact medial malleolus with widened lateral clear space (yellow arrow)
- Scout image(e) demonstrates high level fracture of the fibula (Maisonneuve fracture) that not seen in the CT images (green arrow)

Discussion

Ankle fractures disrupt the osseoligamentous mortise that stabilizes the body of the talus. Fracture patterns include the isolated medial or lateral malleolus, and the bi-malleolar or tri-malleolar fractures with the posterior malleolus formed by the posterior lip of the distal tibia. Fracture dislocations are common, as are avulsion fractures from the malleoli, which represent collateral ligament injuries (5).

The talus is the critical anatomic linkage for a functional ankle. Prompt and accurate diagnosis of talar fractures is crucial to ensure proper management and reduce long term morbidity. Articular cartilage covers 60% of the talus, and the talar blood supply is particularly vulnerable to disruption in talar fracture-dislocation (6).

Our study was consistent with Dale et al. who stated that the most common type of talar fracture was an isolated body fracture (6).

Pilon fractures are among the most complex injuries of the lower limb and their management is technically demanding. Surgical treatment of these fractures is challenging, and creates several difficulties, both in restoration of the articular surface and axial alignment of the tibia and in management of the surrounding (7).

Different investigators identically classified only 38% of fractures of the proximal humerus. Similar results provided studies concerning fractures of the distal radius and distal tibia. Due to these results, it does not seem reasonable to classify complex intra-articular fractures

only by means of conventional radiographs (8).

Computerized tomography (CT) can be used to provide more detailed information about number and displacement of articular fracture fragments with the added benefit of being able to manipulate images to reconstruct 3-dimensional images of the fracture. It has become an integral, validated tool used to plan surgical approach, determine screw sizes, thread length and thin wire placement for hybrid fixators (9).

Leonetti et al. (7) used preoperative CT to classify these fractures based on the number of articular fragments, their dislocation, the zones of comminution and the direction of the major fracture line. These factors represent a key point for the planning and treatment of pilon fracture.

Our study is consistent with Mandracchia et al. (10), as they stated that higher energy injuries such as a fall from a height or motor vehicle collision can produce significant comminution of bone and disruption of the soft tissue envelope and are usually accompanied by a fibular fracture.

Calcaneal fractures: Os calcis fractures are the most frequently fractured tarsal bone accounting for more than 60% of tarsal fractures, and are typically caused by a fall from height (5).

A profound knowledge of the irregular anatomy of the calcaneus and its neighboring bones and a three-dimensional imagination are indispensable in assessing and treating calcaneus fractures (11).

Our study included twenty patients having calcaneal fractures, three patients (15%) of them presented with bilateral calcaneal fractures, where the mechanism of injury

was falling from height in 15 patients (75%), and traffic accidents in 5 patients (25%).

The present study was consistent with Rammelt and Zwipp study, who reported that the vast majority of calcaneal fractures result from heavy deceleration, such as a fall from a height or motor vehicle accidents with the foot pressed firmly against a pedal (11).

In our study, classification was done on basis of axial and coronal images oriented parallel to the posterior facet of the subtalar joint as shown on the sagittal MPR image. The coronal MPR image was the key to depict the number and location of intra-articular fracture lines as well as the degree of displacement of articular fragments, and to finally classify calcaneal fractures.

Rammelt and Zwipp stated that if an intra-articular fracture or major displacement is suspected, CT scans are carried out. These allow for a three-dimensional analysis of fracture morphology and determination of joint involvement and are extremely helpful in planning the surgical approach (11).

Reiger confirmed that axial CT can be challenging when trying to interpret regions of complex anatomy such as ankle and hind foot. For example, the precise localization of the articular facets of the subtalar joints may be difficult to appreciate on routine axial scans. High-resolution reconstructions created from the CT data provide an additional perspective that can improve depiction of the subtalar joint anatomy (8).

Conclusion

MDCT allows for scanning through full plaster casts or back-slabs. The image quality is improved, as the patients are

more comfortable, and they lie still for the duration of the examination. When MPR and 3D VR images are required, it is a simple task to “cut away” the cast using the scalpel tool at the workstation.

With MDCT, it is no longer necessary to position patients who are already in pain into uncomfortable positions in order to obtain diagnostic images.

Routine fractures of the ankle do not require CT. It is recommended in patients showing only fibular fracture with no associated medial malleolar fracture, provided that the fibular fracture is at or above the level of the syndesmosis. MDCT in these cases, may be of help in detection of radiographically occult ligamentous injury.

In complex intra-articular distal tibial fractures, MDCT demonstrates well the degree of articular surface depression, fragment size and position. Data obtained from volume-rendered imaging may assist the clinician in triaging the patient to immediate surgery or later, definitive arthroplasty.

Computed tomography is valuable in the diagnosis of cases of occult syndesmotic injury, especially when the patient cannot tolerate stress radiographs.

Because the vast majority of talar fractures are intra-articular, CT is performed once a talar fracture is suspected, to rule out a minimally displaced fracture or minor step-off in the affected joint(s).

In calcaneal fractures, MDCT is recommended if an intra-articular fracture or major displacement is suspected. This allows for a three-dimensional analysis of fracture morphology and determination of joint involvement and is extremely helpful in planning the surgical approach.

References

1. Haapamaki V V, Kiuru MJ, Koskinen SK. Ankle and foot injuries: analysis of MDCT findings. *Am J Roentgenol.* 2004;183(3):615–22.
2. Koehler S, Eiff P. Overview of ankle fractures in adults. Waltham (MA): UpToDate. 2018;
3. Lugg ST, Howells PA, Thickett DR. Optimal vitamin D supplementation levels for cardiovascular disease protection. *Dis Markers.* 2015;2015.
4. Ohashi K, El-Khoury GY, Bennett DL. MDCT of tendon abnormalities using volume-rendered images. *Am J Roentgenol.* 2004;182(1):161–5.
5. Hopton BP, Harris NJ. Fractures of the foot and ankle. *Surg.* 2003;9(21):236–40.
6. Dale JD, Ha AS, Chew FS. Update on talar fracture patterns: a large level I trauma center study. *Am J Roentgenol.* 2013;201(5):1087–92.
7. Leonetti D, Tigani D. Pilon fractures: a new classification system based on CT-scan. *Injury.* 2017;48(10):2311–7.
8. Rieger M. Clinical Applications of 3D Imaging in Emergencies. In: *Image Processing in Radiology.* Springer; 2008. p. 345–54.
9. Chowdhry M, Porter K. The pilon fracture. *Trauma.* 2010;12(2):89–103.
10. Mandracchia VJ, Evans RD, Nelson SC, Smith KM. Pilon fractures of the distal tibia. *Clin Podiatr Med Surg.* 1999;16(4):743–67.
11. Bartoníček J, Rammelt S, Kostlivý K, Vaněček V, Klika D, Trešl I. Anatomy and classification of the posterior tibial fragment in ankle fractures. *Arch Orthop Trauma Surg.* 2015;135(4):505–16.

To cite this article: Medhat M. Refaat, Ahmed S. Ali, Amr M. Riyadh. Role of Multi-Detector Computed Tomography in Evaluation of Ankle Trauma. *BMFJ* 2023;40 (Radiology):11-22.